and linear polarization by simply changing the orientation angle of dipole. Circularly polarized antenna exhibits higher bandwidth due to asymmetry in the HIS. Linearly polarized antenna shows better cross-polar levels as compared with that designed using symmetrical HIS.

REFERENCES

1. D.F. Sievenpiper, High-impedance electromagnetic surfaces, Ph.D. dissertation at University of California, Los Angeles, 1999.
2. S.R. Best and D.L. Hanna, Design of a broadband dipole in close proximity to an EBG ground plane, IEEE Antennas Propag Mag 50 (2008), 52–64.
3. L. Akhoondzadeh, D.J. Kern, P.S. Hall, and D.H. Werner, Wideband dipoles on electromagnetic bandgap ground planes, IEEE Trans Antennas Propag 55 (2007), 2426–2434.
4. G. Gupta, Low profile RFID antennas using high impedance surfaces, M.Tech Thesis at IIT Kanpur, 2014.
5. F. Yang and R. Samii, Polarization dependent electromagnetic bandgap surfaces: Characterization, designs, and applications, Vol. 3, In: IEEE International Symposium on Antennas and Propagation, Columbus, OH, 2003, pp. 339–342.
6. M.N. Sujatha and K.J. Vinoy, Compact polarization dependent EBG surface with fractal boundary patches, In: IEEE Asia Pacific Conference on Antennas and Propagation, Singapore, 2012.
7. S. Ullah, J.A. Flint, and R.D. Seager, Polarization-dependent electromagnetic band gap incorporating a slanted sheet via, IET Microwaves Antennas Propag 5 (2011), 519–527.
8. G. Gupta and A.R. Harish, A broadband dipole on a double layered via-less high impedance surface, In: IEEE International Symposium on Antennas and Propagation, Memphis, TN, 2003, 1560–1561.
9. B.Y. Toh, R. Cahill, and V.F. Fusco, Understanding and measuring circular polarization, IEEE Trans Educ 46 (2003), 313–318.

A FRACTAL-BASED COMPACT BROADBAND POLARIZATION INSENSITIVE METAMATERIAL ABSORBER USING LUMPED RESISTORS

Praneeth Munaga, Saptarshi Ghosh,
Somak Bhattacharyya, and Kumar Vaibhav Srivastava
Department of Electrical Engineering, Indian Institute of Technology Kanpur, Kanpur 208016, India; Corresponding author: joysaptarshi@gmail.com

ABSTRACT: *In this article, a broadband polarization insensitive metamaterial absorber has been proposed for C-band (4–8 GHz) applications using lumped resistors. The unit cell of the proposed structure is based on an inverted Minkowski fractal loop, where four lumped resistors are mounted to obtain a broad absorption band at the expense of 5 mm thick dielectric substrate, which is only $0.033\lambda_0$ with respect to the lowest operating frequency. The proposed structure is polarization insensitive and also wide angle absorptive. A prototype of the proposed structure has been fabricated, which is experimentally verified with the simulated responses. The designed structure is much compact compared with other reported structures due to its unique design and thus can be considered as a compact broadband absorber for C-band applications.* © 2016 Wiley Periodicals, Inc. Microwave Opt Technol Lett 58:343–347, 2016; View this article online at wileyonlinelibrary.com. DOI 10.1002/mop.29571

1. INTRODUCTION

Day-by-day, there is a tremendous advancement in the utilization of metamaterial characteristics in real time applications like manufacturing of perfect lens [1], cloaking [2], antenna miniaturization [3], absorber [4], and so forth. Because of the unusual electromagnetic (EM) properties of the metamaterials, they are preferred in several applications in various frequency ranges starting from microwave to optical domain. Commercial wedge- and pyramidal-shaped microwave absorbers, used for EM absorption, require large spaces as well as they are bulky [5]. Therefore, there is always a search for ultrathin and light-weight EM absorbers, where the metamaterial based absorbers have come into existence. As the first metamaterial based absorber has been experimentally demonstrated in 2008 by Landy et al. [4], various designs on metamaterial absorbers have been investigated exhibiting different characteristics, such as single-band, dual-band, as well as broadband operations in different spectral ranges [6–10].

A metamaterial absorber generally consists of a periodic array of unit cells, formed by a dielectric substrate sandwiched between the top metallic pattern and bottom ground plane. The structure produces equivalent inductances and capacitances depending on the metallic patches and the gaps between the patches, respectively, which give rise to LC equivalent circuit. This causes dips in reflection and thereby near-unity absorption is obtained at resonance frequencies. As these metamaterial absorber structures are mainly based on resonance mechanism, the structures suffer from narrow absorption bandwidths. Hence many methods like multilayer [11], array of scaled unit cells [12], use of resistive sheet [13], mounting of lumped elements [14] have been proposed to achieve wideband and broadband absorption. Each method has its own advantages and disadvantages. Among them the simpler and cost effective one is the use of lumped resistors, where by appropriately choosing the resistor values, broad absorption band can be realized.

In this article a polarization insensitive and wide angle absorptive broadband absorber has been proposed, which comprises of inverted Mikowski fractal geometry mounted with lumped resistors. The structure exhibits 10-dB absorption bandwidth over the frequency range of 4–8.12 GHz under normal incidence with peak absorptions of 94.4% and 97.7% at 4.82 GHz and 7.84 GHz, respectively. The equivalent circuit model has been drawn to understand the absorption phenomenon. The reflectivity responses of the structure for oblique incidence and for different polarization angles under normal incidence show that the proposed absorber is polarization insensitive in nature as well as it maintains good absorption for angle of incidence upto 60°. Additionally, the structure is fabricated and the experimental responses have been verified with the simulated results. Last, the designed broadband absorber has been compared with other reported structures to show its advantage in terms of its compactness.

2. DESIGN OF THE STRUCTURE

The top layer of the unit cell consists of a first-order inverted Minkowski fractal geometry, which is imprinted on a grounded FR-4 dielectric substrate ($\varepsilon_r = 4.4$ and tan $\delta = 0.02$) of 5 mm thickness as shown in Figure 1(a). Both the top and bottom layers are made of copper ($\sigma = 5.8 \times 10^7$ S/m) of 0.035 mm thickness. The geometric dimensions of the unit cell are as follows: $a = 12.5$, $d = 10.5$, $w = 0.9$, $g_1 = 1.2$, $P = 0.6$, $g_2 = 0.4$, gap $= 1.5$, while the dimensions of chip resistors (R_C) are $w_r = 1.25$ and $l_r = 1.2$ (all are in mm). The chip resistor
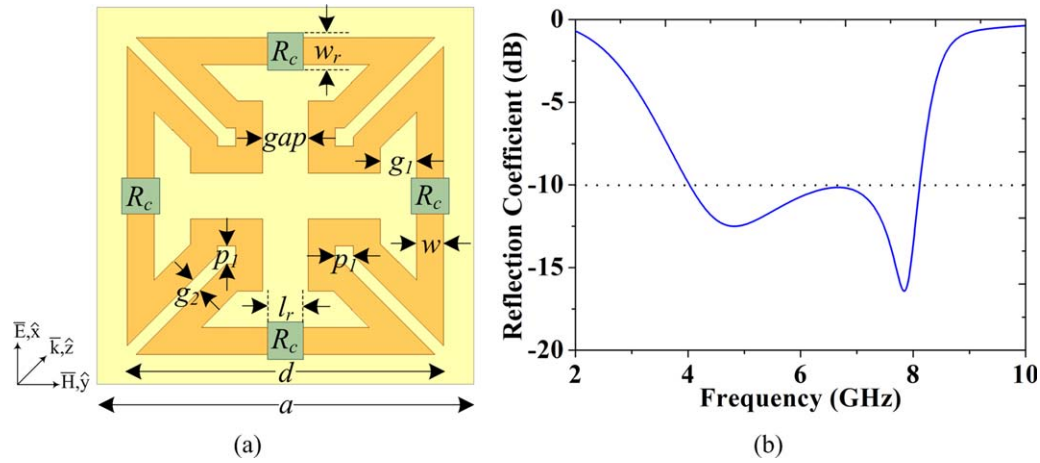
Figure 1 (a) Front view of the unit cell geometry with geometric dimensions: $a = 12.5$, $d = 10.5$, $w = 0.9$, $g_1 = 1.2$, $P = 0.6$, $g_2 = 0.4$, gap = 1.5, $w_r = 1.25$, and $l_r = 1.2$ (units: mm), (b) reflectivity of the simulated structure. [Color figure can be viewed in the online issue, which is available at wileyonlinelibrary.com]

dimensions are chosen according to technical data sheet of the resistors used in fabricated sample. The lumped resistors have the value of 150 Ω. The direction of incident EM wave is normal to the plane of unit cell geometry, which along with the electric and magnetic field vector directions are shown in Figure 1(a).

The structure is simulated in finite element method-based EM solver Ansys HFSS using periodic boundary conditions. Figure 1(b) shows the reflectivity of the structure under normal incidence, where the reflection coefficient is less than −10 dB over the frequency range 4–8.12 GHz covering the entire C-band. Two reflection dips are also observed at frequencies 4.82 GHz and 7.84 GHz with reflection coefficients of −12.5 dB and −16.42 dB, respectively.

When an EM wave is incident on a structure with complete copper backing, the relation between absorptivity and reflectance can be written as in (1):

$$A(\omega) = 1 - |S_{11}(\omega)|^2 \qquad (1)$$

where $A(\omega)$, $|S_{11}(\omega)|^2$ are the absorbance and reflectance, respectively, at an angular frequency ω. This reflection coefficient can be calculated from (2):

$$S_{11} = \frac{Y_0 - Y_{in}}{Y_0 + Y_{in}} \qquad (2)$$

where Y_0 and Y_{in} are the admittance of air and the input admittance of the structure, respectively, which are shown in the equivalent circuit representation of the structure designated as Figure 2(a).

This equivalent circuit of the proposed absorber consists of a frequency selective surface (FSS) based metallic pattern on the top surface, which can be modelled as a RLC series circuit and a transmission line formed by the dielectric substrate terminated by metal ground plane. Therefore, the input admittance of the structure can be represented as follows:

$$Y_{in} = Y_{FSS} + Y_d \qquad (3)$$

where

$$Y_{FSS} = \frac{1}{R_{eff} + j\omega L_{eff} - \frac{j}{\omega C_{eff}}} = G + jB \qquad (4)$$

$$G = \frac{\omega^2 R_{eff} C^2_{eff}}{\omega^2 R^2_{eff} C^2_{eff} + (1 - \omega^2 L_{eff} C_{eff})^2} \qquad (5)$$
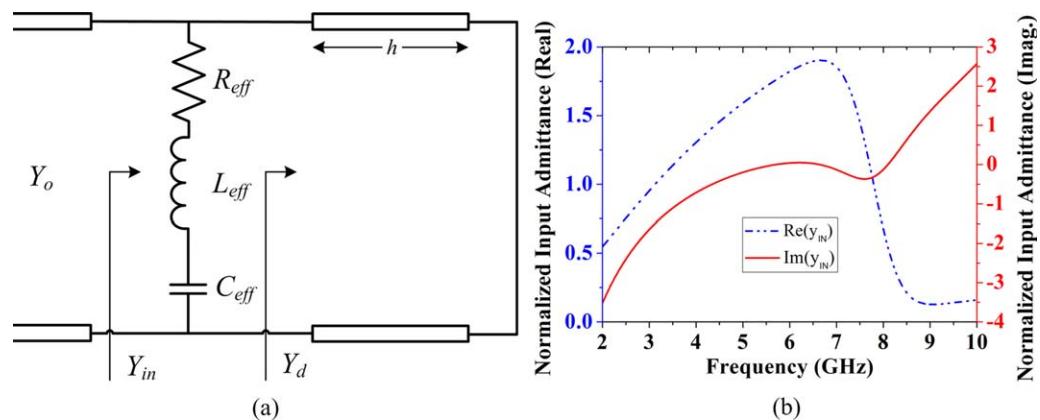

Figure 2 (a) Equivalent circuit model and (b) normalized input admittance of the proposed structure. [Color figure can be viewed in the online issue, which is available at wileyonlinelibrary.com]
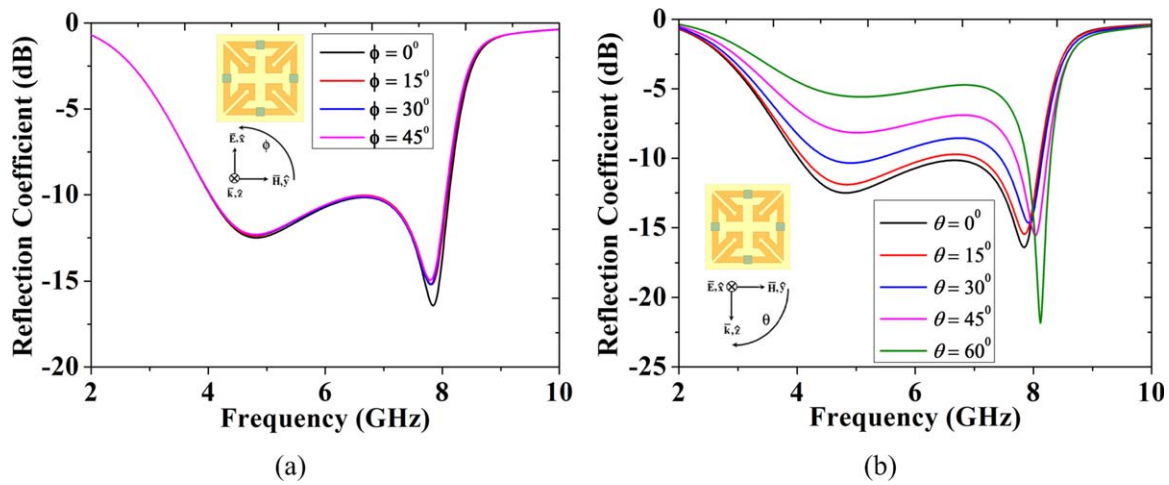
Figure 3 Reflectivity of the simulated structure (a) for different polarization angles of incident wave under normal incidence and (b) for different incident angles under TE polarization. [Color figure can be viewed in the online issue, which is available at wileyonlinelibrary.com]

$$B = \frac{\omega C_{\text{eff}}(1 - \omega^2 L_{\text{eff}} C_{\text{eff}})}{\omega^2 R^2_{\text{eff}} C^2_{\text{eff}} + (1 - \omega^2 L_{\text{eff}} C_{\text{eff}})^2} \tag{6}$$

$$Y_{\text{d}} = -j\sqrt{\varepsilon_0 \varepsilon_{\text{r}} / \mu_0 \mu_{\text{r}}} \cot(kh) \tag{7}$$

where ε_{r} and μ_{r} are the relative permittivity and permeability of the dielectric substrate, respectively, while k being the wave number of the incident EM wave in the dielectric medium which in turn can be written as $k = k_0\sqrt{\varepsilon_{\text{r}}\mu_{\text{r}}}$.

When an EM wave is incident on any interface separating two media, the reflection and transmission of the wave are mainly governed by the intrinsic impedances of the two media. If there is no transmission due to complete metal backing, the absorption of the incident wave in the second medium can be maximized by minimizing the reflectivity only and that can be possible by proper admittance matching at the interface as observed from (2). As the input admittance (Y_{in}) of the proposed structure is the parallel combination of the top FSS admittance (Y_{FSS}) and the terminated dielectric admittance (Y_{d}), the susceptance of Y_{FSS} has to be cancelled out by the susceptance of Y_{d} to make the overall admittance (Y_{in}) real and only then the input

admittance will match the free space admittance, thus causing near-unity absorption as observed from (3)–(7).

The real and imaginary parts of the normalized input admittance (calculated from simulated reflection coefficient) are plotted in Figure 2(b) and it is observed that Im(y_{IN}) to be close to 0 for the entire frequency range of 4–8.12 GHz thus satisfying the above conditions for admittance matching. Although the proposed structure provides two reflection dips, one below the Salisbury screen zone and another above the Salisbury screen zone [13], the observed bandwidth is very large instead of two narrow absorption peaks at these two frequencies (4.82 and 7.84 GHz). This broad absorption band has been realized by the surface mounting lumped resistors, where the resistors absorb the incident EM wave energy, thus realizing broadband.

The proposed absorber is four-fold symmetric by design and, therefore, polarization insensitive as verified from Figure 3(a). The reflectivity of the structure is further studied for different incident angles upto 60° under transverse electric (TE) polarization as shown in Figure 3(b), which exhibits good absorption ($|S_{11}| < -7.5$ dB) upto 45° angle of incidence.

To examine the effect of the chip resistors on the designed absorber, the simulated reflection coefficients for different values of resistors are plotted in Figure 4. It is observed that as the resistance value increases, the full width at half maximum bandwidth of the structure decreases gradually. This can be explained from the parallel resonant circuit shown in Figure 2(a), where the quality factor (Q) of the structure increases proportionally with the resistance value (R_{eff}). However, the reflection coefficient of the structure gradually increases with decreasing value of resistors. Therefore, an optimum value of resistor ($R_{\text{C}} = 150$ Ω) has been chosen which gives rise to wide absorption bandwidth as well as maintains -10 dB reflection level throughout the desired frequency range.
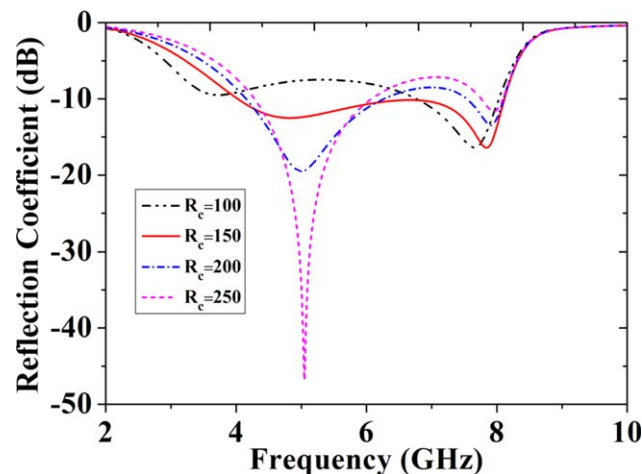
3. EXPERIMENTAL RESULTS

To experimentally verify the proposed broadband absorber, the structure is fabricated on the top surface of FR-4 substrate having dimensions of 175 mm × 175 mm × 5 mm with complete copper lamination at back. Then the chip resistors of 150 Ω are soldered on the fabricated design in surface-mounting technology. The fabricated structure, consisting of 14 × 14 unit cells and a total of 784 chip resistors, is depicted in Figure 5(a) along with its enlarged view.
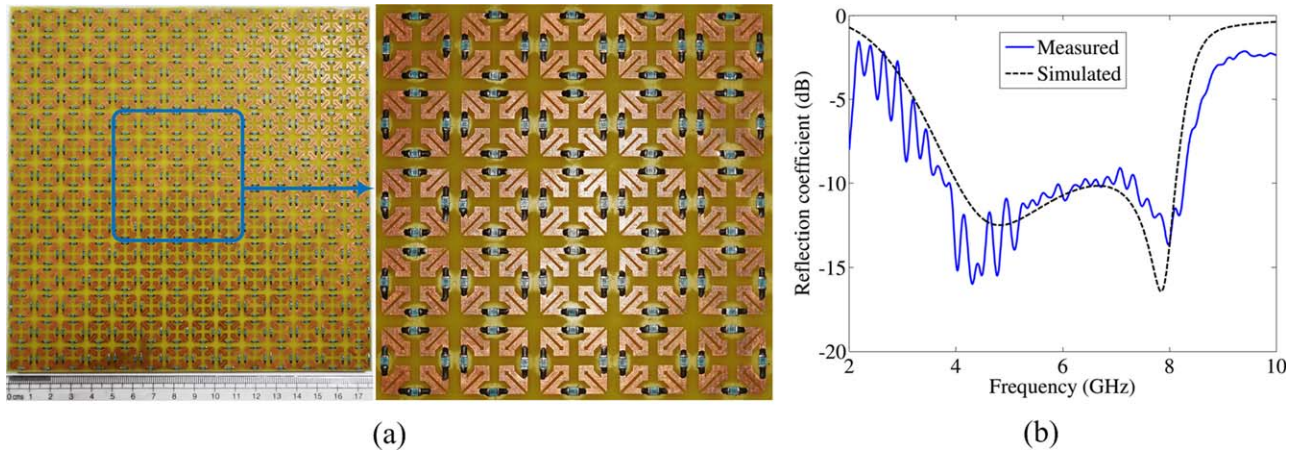

Figure 4 Reflection coefficient for different chip resistor (R_{C}) values of the proposed broadband absorber. [Color figure can be viewed in the online issue, which is available at wileyonlinelibrary.com]

Figure 5 (a) Photograph of the fabricated absorber with enlarged view showing 5 × 5 array of unit cells, and (b) comparison of the simulated and measured reflection coefficients of the proposed broadband absorber structure. [Color figure can be viewed in the online issue, which is available at wileyonlinelibrary.com]
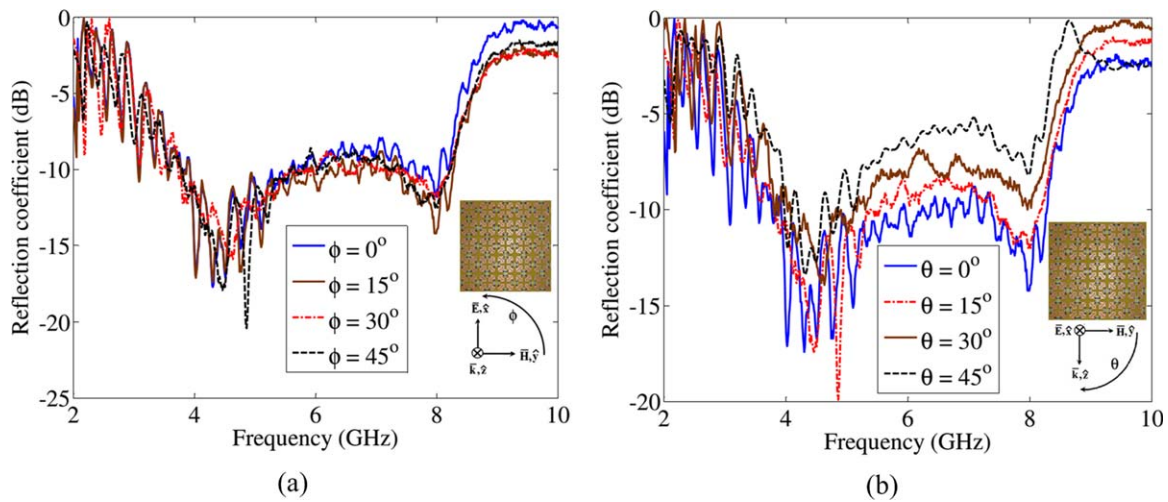

Figure 6 Measured reflection coefficients of the fabricated structure for different angles of (a) polarization under normal incidence and (b) oblique incidence under TE polarization. [Color figure can be viewed in the online issue, which is available at wileyonlinelibrary.com]
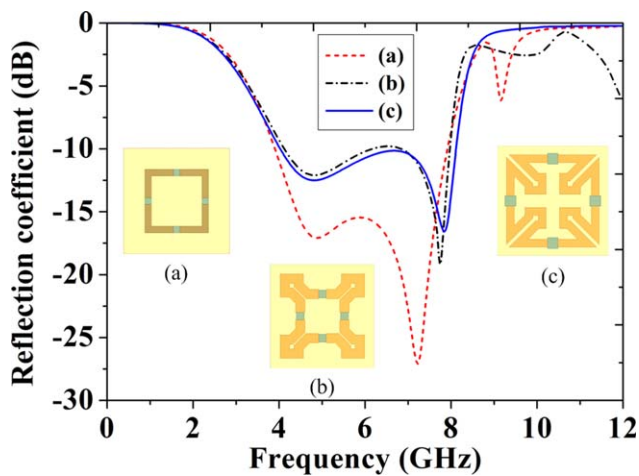

Figure 7 Comparison of reflection coefficients among different shaped broadband absorbers: (a) Single square loop, (b) Minkowski geometry, and (c) Proposed one. [Color figure can be viewed in the online issue, which is available at wileyonlinelibrary.com]

A pair of broadband (1–18 GHz) horn antennas is used along with Agilent N5230A network analyzer to measure the reflections from the fabricated sample. The distance between the structure and the antenna pair is adjusted so that far-field condition is maintained throughout the experiment and the whole experiment set up is placed inside the anechoic chamber. Initially, the reflection coefficient from a metal plate of identical dimension has been recorded and stored as a reference value. Then the reflection from the fabricated structure has been measured and the difference between the two reflected values gives the actual reflection coefficient of the structure. This differential measurement process minimizes the edge diffraction, path loss and any other anomaly present in the measurement process. The measured reflectivity is observed in Figure 5(b), which is below −10 dB for the frequency range of 3.78–8.28 GHz covering the entire C-band. Two minima are also observed at 4.31 and 7.98 GHz, with reflection coefficients of −15.97 and −13.64 dB, respectively.

The fabricated structure is examined for its polarization insensitive behavior under normal incidence by rotating the sample around its own axis in steps of 15° upto 45° and the

TABLE 1 Summary of design, geometry and size

Absorber Designs	Centre Frequency (GHz)	Unit Cell Size (mm)	Thickness (mm)	−10 dB Bandwidth (GHz)
Single square loop (a)	6	20 ($0.4\lambda_0$)	6 ($0.12\lambda_0$)	4–8
Minkowski geometry (b)	6.05	16.5 ($0.33\lambda_0$)	5 ($0.10\lambda_0$)	4.12–7.97
Proposed one (c)	6.06	12.5 ($0.25\lambda_0$)	5 ($0.10\lambda_0$)	4.03–8.11

reflection coefficient is found to be almost similar in each case as observed from Figure 6(a). Finally, the reflectivity of the structure for different incident angles under TE polarization is measured and is depicted in Figure 6(b), which validates the simulated results in good agreement.

4. CONCLUSION

A broadband ultrathin metamaterial absorber has been presented based on lumped resistors. The proposed design is polarization insensitive, wide angle absorptive (upto 45°for TE polarization) and the absorption range covers the entire C-band (4–8.12 GHz) with above 90% absorption level. The absorber has been fabricated and the simulated responses have been verified with the measured results. The proposed design is based on first-order Minkowski fractal geometry, where the tetra arrows have been inverted to make the geometry compact. The proposed structure has also been compared with other broadband absorbers (standard single square loop and Minkowski fractal geometry) operating in C-band as shown in Figure 7 and the compactness of the designed geometry has been clearly observed in Table 1. Therefore, the proposed absorber can be used in several potential applications like radar cross section (RCS) reduction, shielding and in electromagnetic interference/electromagnetic compatibility where the installation dimensions can be significantly reduced.

REFERENCES

1. N. Fang, H. Lee, C. Sun, and X. Zhang, Sub-diffraction-limited optical imaging with a silver superlens, Science 308 (2005), 534–537.
2. D. Schurig, J.J. Mock, B.J. Justice, S.A. Cummer, J.B. Pendry, A.F. Starr, and D.R. Smith, Metamaterial electromagnetic cloak at microwave frequencies, Science 314 (2006), 977–980.
3. S. Enoch, G. Tayeb, and P. Vincent, A metamaterial for directive emission, Phys Rev Lett 89 (2002), 3901–3904.
4. N.I. Landy, S. Sajuyigbe, J.J. Mock, D.R. Smith, and W.J. Padilla, Perfect metamaterial absorber, Phys Rev Lett 100 (2008), 207402.
5. K.J. Vinoy and R.M. Jha, Radar absorbing materials: From theory to design and characterization, 1st ed., Kluwer, Norwell, MA, 1996.
6. H. Tao, N.I. Landy, C.M. Bingham, X. Zhang, R.D. Averitt, and W.J. Padilla, A metamaterial absorber for the terahertz regime: Design, fabrication and characterization, Opt Express 16 (2008), 7181–7188.
7. Q.Y. Wen, H.W. Zhang, Y.S. Xie, Q.H. Yang, and Y.L. Liu, Dual band terahertz metamaterial absorber: Design, fabrication and characterization, Appl Phys Lett 95 (2009), 241111.
8. S. Bhattacharyya, S. Ghosh, and K.V. Srivastava, Triple band polarization-independent metamaterial absorber with bandwidth-enhancement at X-band, J Appl Phys 114 (2013), 094514.
9. S. Ghosh, S. Bhattacharyya, Y. Kaiprath, and K.V. Srivastava, Bandwidth-enhanced polarization insensitive microwave metamaterial absorber and its equivalent circuit, J Appl Phys 115 (2014), 104503.
10. S. Gu, B. Su, and X. Zhao, Planar isotropic broadband metamaterial absorber, J Appl Phys 114 (2013), 163702.
11. H. Xiong, J.-S. Hong, C.-M. Luo, and L.-L. Zhong, An ultrathin and broadband metamaterial absorber using multi-layer structures, J Appl Phys 114 (2013), 064109.
12. S. Ghosh, S. Bhattacharyya, and K.V. Srivastava, Bandwidth-enhanced of an ultra-thin polarization insensitive metamaterial absorber, Microwave Opt Technol Lett 56 (2014), 350–355.
13. F. Costa, A. Monorchio, and G. Manara, Analysis and design of ultrathin electromagnetic absorbers comprising resistively loaded high impedance surfaces, IEEE Trans Antennas Propag 58 (2010), 1551–1558.
14. J. Yang and Z. Shen, A thin and broadband absorber using double-square loops, IEEE Antennas Wireless Propag Lett 6 (2007), 388–391.

A 460-GHz CMOS SUBSTRATE-INTEGRATED-WAVEGUIDE SLOT-ANTENNA DESIGN

Hao Xie, Leonid Belostotski, and Michal Okoniewski
Department of Electrical and Computer Engineering, University of Calgary, Calgary, Canada; Corresponding author: lbelosto@ucalgary.ca

ABSTRACT: *A design of a 460 GHz substrate-integrated-waveguide (SIW) slot antenna in a 65-nm CMOS process is presented in thisarticle. The size of the antenna is 380 μm × 224 μm. An inductor identification layer is placed in the layout to reduce the internal metal density requirements significantly. The proposed antenna, which includes metal dummy fill to be compliant with the 65 nm process design rules, was simulated using HFSS. The antenna simulated with a 0.5 mm Si substrate has a maximum gain of 0.09 dBi and a radiation efficiency of 29.1%. The bandwidth of S_{11} below −10 dB is 25.3 GHz. © 2016 Wiley Periodicals, Inc. Microwave Opt Technol Lett 58:347–351, 2016; View this article online at wileyonlinelibrary.com. DOI 10.1002/mop.29570*

1. INTRODUCTION

Cerro Chajnantor Atacama Telescope (CCAT) will be a next-generation sub-millimeter telescope, which is a 25-m telescope located at 5600 m altitude on Cerro Chajnantor, in the Atacama desert of northern Chile [1]. One of the first-light instruments for CCAT is the CCAT Heterodyne Array Instrument (CHAI), which is a dual-frequency band array receiver covering the scientifically most important parts of the 460 and 830 GHz atmospheric windows for simultaneous observations with 64-pixel arrays. This work is a pilot project to investigate the feasibility of a design of a 460 GHz on-chip antenna with the purpose of integrating with entire CHAI receiver on the same integrated circuit. While this work is not officially a part of CCAT CHAI development, it may provide alternatives to cost-effective implementation of CHAI.

There are many different kinds of THz on-chip antennas emerging in the past years: slot [2], dipole [3], patch [4], Yagi-Uda [5], ring [6], and so on. A 434-GHz substrate-integrated-waveguide (SIW) slot antenna with a transmitter/receiver chipset was fabricated in SiGe BiCMOS process, which had a simulated gain of −0.55 dBi and efficiency of 49.8% [2]. A 0.54-THz